2008 IEEE International Conference on
Robotics and Automation
Pasadena, CA, USA, May 19-23, 2008

Control of a Mobile Haptic Interface

Ulrich Unterhinninghofen, Thomas Schauß, and Martin Buss
Institute of Automatic Control Engineering
Technische Universität München
D-80290 München, Germany
ulrich.unterhinninghofen@tum.de, thomas.schauss@mytum.de, m.buss@ieee.org

***Abstract*— The hardware and control concept of a mobile haptic interface is presented. It is intended to provide spatially unrestricted, dual-handed haptic interaction. The device is composed of two haptic displays mounted on an omnidirectional mobile base which is controlled in such a way that the haptic displays are not driven to their workspace limits. A simple algorithm, based on end-effector positions only, and a more sophisticated approach, incorporating also the body position of the operator, are presented and compared. Experimental results show that the latter algorithm performs better in most use cases.**

I. INTRODUCTION

A. Motivation

A haptic interface mediates positions and forces between a human operator and a telepresent or virtual environment. Consequently, it must be able to sense the poses of the human hands and exert forces on the hands at the same time. In numerous application domains, e.g. telepresent maintenance work or virtual shopping, the user is expected to walk around in the target environment. Hence, the desired workspace is far larger than the reach of the human arm. The workspace covered by typical haptic interfaces, however, is even much smaller than the full reach of the human arm. In order to enable haptic interaction in spatially unlimited environments, an alternative approach must be chosen.

To this end, two haptic displays have been mounted on a mobile base. When the position of the mobile base is controlled in such a way that the end-effectors of both haptic displays are kept far from the limits of their respective workspaces, the operator can move around freely while the mobile base actively follows his motions. The typical scheme of operation is illustrated in Fig. 1: the human operator holds the end-effectors of the haptic displays which are used to track positions and exert forces. The combined position data from haptic displays and mobile base are sent to a virtual avatar or mobile teleoperator which implements the given movements in the target environment. A picture of the complete system is shown in Fig. 2.

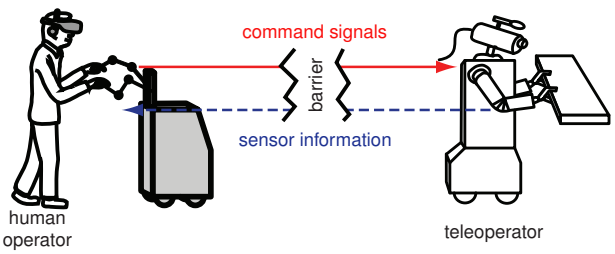

Fig. 1. Concept of a Mobile Haptic Interface (MHI): a human operator holds the end-effector of two haptic displays mounted on a mobile base. The position and force signals can be used to drive a virtual avatar or mobile teleoperator.

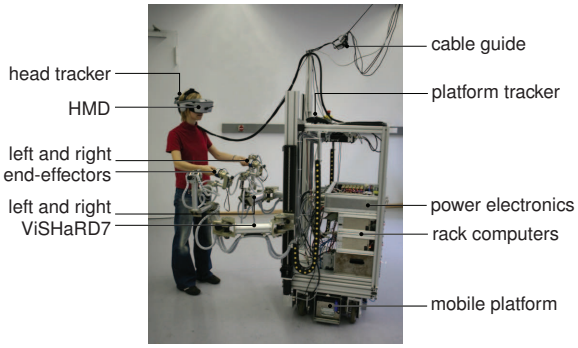

Fig. 2. Hardware setup in a typical application scenario

B. State of the Art

The easiest way to make haptic interaction in large environments possible is to use additional input devices, e.g. joysticks or pedals, to control the locomotion of the teleoperator or virtual avatar. However, this method does not provide a natural sensation of the locomotion and compromises the navigation skills of the operator [1]. Different devices have been developed to overcome these limitations. The most relevant are ground-based and body-based haptic interfaces [2]. Stationary, i.e. ground-based, haptic interfaces normally do not provide a truly unrestricted workspace. This can be compensated by combining them with a treadmill, which can convey a good impression of the travelled distance, but does not perform well on curved paths. Body-based haptic interfaces are worn by the user, thus providing an unlimited workspace. However, the operator has to support the full load of the haptic interfaces, which is very fatigueing.

Mobile haptic interfaces can cope with both drawbacks, because the self-motion of the operator is used to derive the desired motion of teleoperator or avatar, and the weight of the display is supported by the mobile base. The concept has been presented in [3] for a single-handed haptic interface with four degress of freedom. An implementation of a dual-handed and mobile haptic interface is published in [4].

However, the hardware and control design of the latter device does not allow fast hand motions, because the workspace of the employed Phantom devices is too small and no prediction of future hand motions is made.

C. Contribution

The specific challenge of the control design of the mobile haptic interface is the identification of the optimal position for the mobile base. In existing solutions, it is solely derived from the position of the end-effectors. However, taking the position and orientation of the human operator into account, yields an estimate of future hand positions and can significantly improve performance as shown in this paper. Two control algorithms are compared for two different use cases.

In Sec. II the hardware setup of the mobile haptic interface is presented. A detailed description of the controller design is given in Sec. III. Experimental results are shown in Sec. IV. Finally, a summary and outlook can be found in Sec. V.

II. SETUP

The mobile haptic interface is built out of two haptic displays ViSHaRD7 and an omnidirectional mobile base. ViSHaRD7 is a custom-made, compact haptic display whose workspace covers a half-cylinder with a radius and height of approx. 0.60 m each; it provides peak forces of approx. 150 N. Therefore, ViSHaRD7 is well suited to cover the haptic interaction of a stationary human operator. As can be seen from the kinematic structure illustrated in Fig. 3, translational and rotational degrees of freedom are kinematically decoupled. This facilitates the control of ViSHaRD7 itself, as well as the coordinated motion with the mobile base. Each ViSHaRD7 is equipped with a six degrees of freedom force/torque sensor. The joint angles are sensed by incremental encoders. For a detailed description the reader is referred to [5].

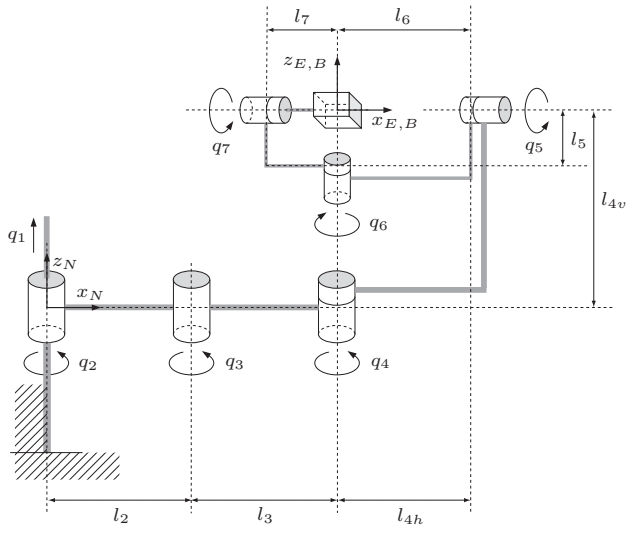

Fig. 3. Kinematic model of ViSHaRD7. Joints $q_1 \dots q_3$ determine the translational part, joints $q_4 \dots q_7$ the rotational part of the end-effector pose.

The two haptic displays are mounted at the front-left and front-right corner of a mobile base. The mobile base must possess omnidirectional manoeuvrability so that it can follow all motions of the human operator. Generally, a holonomic design is favorable because it provides all three planar velocity degrees of freedom at any instant. However, most holonomic drive concepts rely on some sort of "omni-wheel" which are known to create intensive vibrations. Therefore, an alternative non-holonomic design, based on four independently driven and steered wheels (powered caster wheels), is preferred. Although this approach imposes some delays in direction changes, because all wheels must be turned before accelerating in the new direction, it offers a good compromise between manoeuvrability and smooth motions. The mobile base has a maximum payload of approx. 200 kg, which enables it to carry control hardware and large battery packs in addition to the two haptic displays. Details can be found in [6].

III. CONTROL DESIGN

A. Overall Control Structure

The overall control structure of the mobile haptic interface is depicted in Fig. 4. The admittance controllers of both haptic displays translate the end-effector forces and torques into desired end-effector poses. The admittance control law is calculated in world coordinates so that repositioning of the mobile base does not affect the end-effector positions. The actual end-effector positions are used to derive the optimal position of the mobile base. The position is optimal when it provides the operator with maximum manipulability at all times. As this optimal position is calculated in the base coordinate system, it represents a relative position which can be easily transformed to the desired velocity of the mobile base by a linear PD-controller. Finally, the desired velocity is fed to the velocity controller of the mobile base which calculates appropriate control inputs for each wheel.

In order to simplify the optimization problem, only the planar degrees of freedom are considered. This is possible because the mobile base can only perform planar motions, i.e. translations in x– and y–direction and rotations around the z–axis. Furthermore, the planar degrees of freedom are also decoupled in the kinematics of the haptic interfaces (cf. Fig. 3). Consequently, only the joint angles q_2 and q_3 of both arms are needed to compute the optimal relative base position.

B. Manipulability Measure

When maximizing the manipulability of the haptic interfaces, different types of manipulability and different manipulability measures can be considered. Most importantly, one can distinguish between force manipulability and velocity manipulability. In the former case, the configuration dependent ability to exert forces is measured, whereas in the latter case the ability to generate velocity is described. In a device with serial kinematics such as ViSHaRD7, the force manipulability cannot degenerate. In contrast, the velocity manipulability degenerates close to singular configurations (see [7]). Therefore, the optimization strategy is designed to maximize the velocity manipulability of the haptic displays.

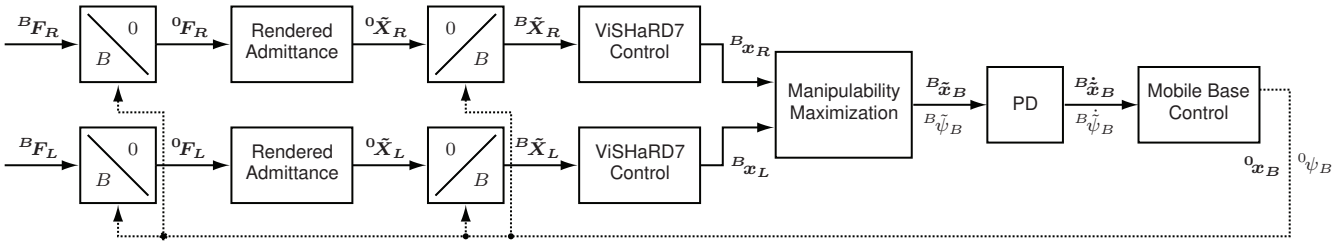

Fig. 4. Overall control structure. ${}^{B}\boldsymbol{F}_{\boldsymbol{R/L}}$ and ${}^{0}\boldsymbol{F}_{\boldsymbol{R/L}}$ denote forces and torques at the end-effectors in base and world coordinates, respectively. ${}^{0}\tilde{\boldsymbol{X}}_{\boldsymbol{R/L}}$ and ${}^{B}\tilde{\boldsymbol{X}}_{\boldsymbol{R/L}}$ describe desired end-effector poses. ${}^{B}\boldsymbol{x}_{\boldsymbol{R/L}}$ are the actual end-effector positions. ${}^{B}\tilde{\boldsymbol{x}}_{\boldsymbol{B}}$, ${}^{B}\tilde{\psi}_{B}$ and ${}^{B}\dot{\tilde{\boldsymbol{x}}}_{\boldsymbol{B}}$, ${}^{B}\dot{\tilde{\psi}}_{B}$ describe desired, relative base position and base velocity, respectively. The estimated position and orientation of the mobile base are denoted ${}^{0}\boldsymbol{x}_{\boldsymbol{B}}$, ${}^{0}\psi_{B}$.

To this end, a manipulability measure based on a singular value decomposition of the Jacobian is used.

The manipulability of the haptic interfaces is bounded by the maximum joint velocities. The resulting maximum velocities in Cartesian space are computed using the Jacobian $\boldsymbol{J}(q_2, q_3)$ of the SCARA part of ViSHaRD7. The smallest singular value $\sigma_m(q_2, q_3)$ of $\boldsymbol{J}(q_2, q_3)$ is commonly used as a measure of manipulability. It describes how fast the end-effector can move in an arbitrary direction without allowing the joint velocities (q_2, q_3) to leave a unit circle. Therefore, maximizing the smallest singular value $\sigma_m(q_2, q_3)$ also maximizes the allowable Cartesian velocity of the end-effector.

The Jacobian is defined by:

$$\boldsymbol{J} = \begin{pmatrix} \frac{\delta x}{\delta q_2} & \frac{\delta x}{\delta q_3} \\ \frac{\delta y}{\delta q_2} & \frac{\delta y}{\delta q_3} \end{pmatrix} \tag{1}$$

$$= \begin{pmatrix} -l_2\sin(q_2) - l_3\sin(q_2+q_3) & -l_3\sin(q_2+q_3) \\ l_2\cos(q_2) + l_3\cos(q_2+q_3) & l_3\cos(q_2+q_3) \end{pmatrix} \tag{2}$$

In order to calculate the maximum Cartesian velocities with respect to the given maximum joint velocities $\dot{q}_{2,max}, \dot{q}_{3,max}$, a scaled Jacobian is used:

$$\boldsymbol{R} = \mathrm{diag}(\dot{q}_{2,max}, \dot{q}_{3,max}), \tag{3}$$

$$\tilde{\dot{\boldsymbol{q}}} = \boldsymbol{R}^{-1}\dot{\boldsymbol{q}} \text{ , where } \boldsymbol{q} = (q_2, q_3)^T, \tag{4}$$

$$\boldsymbol{J}\dot{\boldsymbol{q}} = (\boldsymbol{J}\boldsymbol{R})\tilde{\dot{\boldsymbol{q}}} = \tilde{\boldsymbol{J}}\tilde{\dot{\boldsymbol{q}}}, \tag{5}$$

$$\tilde{\boldsymbol{J}} = \boldsymbol{J}\boldsymbol{R} = \boldsymbol{J}\begin{pmatrix} \dot{q}_{2,max} & 0 \\ 0 & \dot{q}_{3,max} \end{pmatrix}. \tag{6}$$

The smallest singular value $\tilde{\sigma}_m(q_2, q_3)$ of the scaled Jacobian $\tilde{\boldsymbol{J}}(q_2, q_3)$ is the maximum speed with which the manipulator can move in an arbitrary horizontal direction while the joint velocities stay within the given constraints.

Fig. 5 shows the planar velocity manipulability $\tilde{\sigma}_m(\boldsymbol{x})$ of one ViSHaRD7 for all reachable end-effector positions. It is affected by angle q_3, only. Thus, the manipulability is constant on circles around joint 2 and the maximum manipulability is given on a circle with $r_{opt} = 42$ cm.

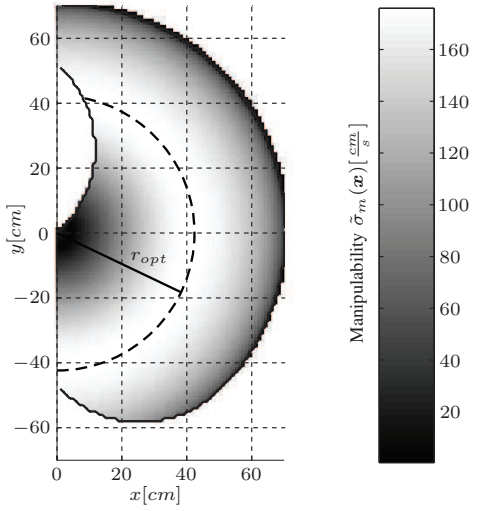

Fig. 5. Manipulability and circle with maximum manipulability in the shoulder coordinate system of ViSHaRD7. On the dashed circle the manipulability $\tilde{\sigma}_m(\boldsymbol{x})$ is maximized.

C. Maximizing Manipulability

As shown in the previous section, the manipulability is optimal when the end-effector position is located on a circle with radius r_{opt}. This criterion yields a solution for the optimal q_3 of both haptic interfaces. Additionally, q_{R2} and q_{L2} should be chosen in such a way that their minimum distance to the joint limits is maximized. This is achieved when both joint angles, q_{R2} and q_{L2}, are equal. The resulting configuration is symmetric and the corresponding base position can be obtained by simple geometric calculations: the mobile base must be aligned parallel to the connecting line from x_L to x_R and its center point must lie on the perpendicular bisector of the connecting line (see Fig. 6).

The end-effector positions $\boldsymbol{x_L}$ and $\boldsymbol{x_R}$ are used to compute the connecting vector $\boldsymbol{d}$ and midpoint $\boldsymbol{x_M}$:

$$\boldsymbol{d} = \boldsymbol{x_R} - \boldsymbol{x_L}, \tag{7}$$

$$\boldsymbol{x_M} = \frac{\boldsymbol{x_R} + \boldsymbol{x_L}}{2}. \tag{8}$$

The vector from the optimal position $\tilde{\boldsymbol{x}}_{\boldsymbol{B}}$ to the midpoint $\boldsymbol{x_M}$ is obtained by calculating its direction which is perpendicular to $\boldsymbol{d}$ pointing away from the mobile base and the optimal distance n_{opt}:

$$\boldsymbol{n} = \frac{\boldsymbol{d}}{\|\boldsymbol{d}\|} \times \boldsymbol{e_z} \tag{9}$$

$$n_{opt} = \sqrt{r_{opt}^2 - \left(\frac{\|\boldsymbol{d}\| - d_P}{2}\right)^2} + n_P \tag{10}$$

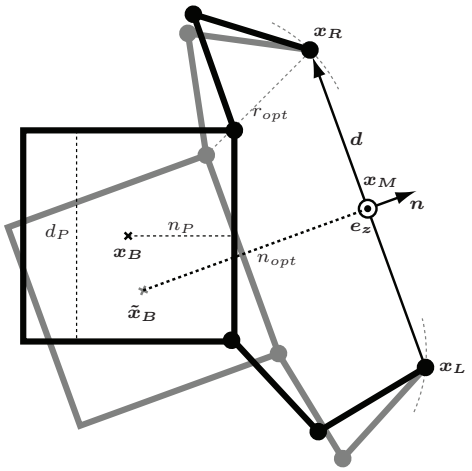

Fig. 6. Geometric solution for optimal mobile base positioning

Finally, the optimal base position $\tilde{\boldsymbol{x}}_{\boldsymbol{B}}$ is calculated:

$$\tilde{\boldsymbol{x}}_{\boldsymbol{B}} = \boldsymbol{x}_{\boldsymbol{M}} - n_{opt} \cdot \boldsymbol{n} \tag{11}$$

As the mobile base can only perform planar motions, the z-component of $\tilde{\boldsymbol{x}}_{\boldsymbol{B}}$ is ignored. The optimal base orientation $\tilde{\psi}_B$ is identical to the direction of the normal vector $\boldsymbol{n}$:

$$\tilde{\psi}_B = \angle \boldsymbol{n} \tag{12}$$

D. Including Human Arm Workspace in Optimization Strategy

The approach presented in the previous section always converges to a configuration of the haptic interfaces which provides the operator with the maximum velocity manipulability. This solution works well for slow motions of the operator where the dynamics of the mobile base can be neglected. In this case, the end-effector positions will always be close to the points of optimal manipulability. For fast operator motions, however, the mobile base cannot reposition the haptic interfaces fast enough to avoid a significant degradation of the manipulability. For even faster motions, the end-effectors can reach the boundaries of the admissible workspace.

It is, therefore, desirable to take the different dynamics of human motions into consideration. Analogously to the motions of the mobile haptic interface, human motions can be decomposed into fast motions of limited range which are performed by using the arms only and slower, but unlimited motions performed by using the legs. According to this idea, the mobile base should be always positioned in such a way that the current workspace of the human arms is mostly covered by the workspace of the two haptic interfaces. This optimization goal requires maximizing the overlap between the workspaces of the human arms and the haptic interfaces. However, this optimization problem cannot be solved in real-time due to its high complexity. Therefore, a simplified approach to take the human workspace into account is presented. Fig. 7 shows the computed workspace of the human arm based on a physiological model (see [8]). The relevant workspace can be well approximated by a semicircle.

In order to increase the overlap between the workspaces of operator arm and corresponding haptic display, the end-effector position used as input for the optimization algorithm presented in Sec. III-C is shifted towards the center of the human workspace $\boldsymbol{x}_{\boldsymbol{C}}$. The effective end-effector positions are calculated by a linear mapping:

$$\boldsymbol{x'} = \boldsymbol{x} + \boldsymbol{S}(\boldsymbol{x}_{\boldsymbol{C}} - \boldsymbol{x}), \quad \boldsymbol{S} = \mathrm{diag}(s_x, s_y) \tag{13}$$

In Fig. 7 the shift from actual end-effector position to effective position is illustrated for shift factors of $s_x = 0.57, s_y = 0.4$. The more the positions are shifted towards the center, the less the mobile base will move when the end-effector positions are changed. In this way, the optimization algorithm can be adjusted to the application by choosing the appropriate shift factors: if the dynamics of the arm motions by far exceed the dynamics of the body motions, high shift factors must be chosen; if, however, highly dynamic body motions can be anticipated, the shift factors should be kept low.

The advantage of this approach can be seen in Fig. 8: In condition a), the operator holds the end-effectors close to his body. Consequently, his arms can only perform small position changes away from the mobile base, but large position changes towards the mobile base. To account for this asymmetry, the mobile base is positioned farther away from the end-effectors. Condition c) shows the opposite condition, where the operator arms are fully extended and the haptic interface is positioned closer to the end-effectors. Condition b) represents the nominal case where actual and shifted end-effector positions are coincident.

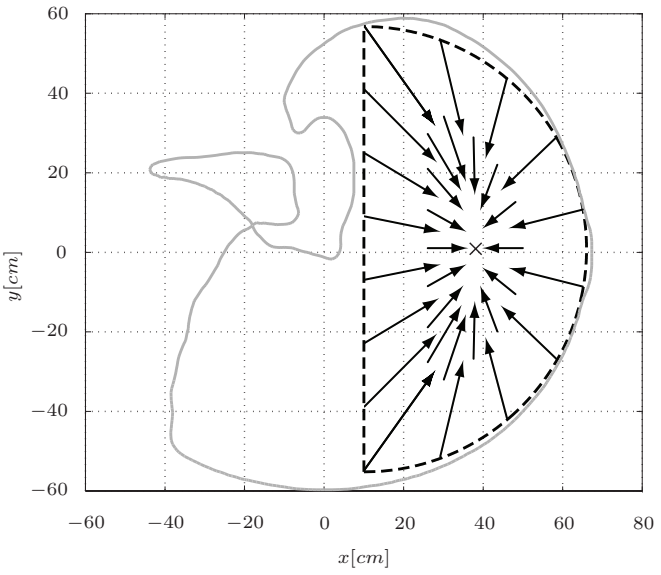

Fig. 7. Workspace of human right arm at shoulder height (solid line) and approximation by a semicircle (dashed line), where the origin is coincident with the right shoulder. The arrows show how end-effector positions are shifted towards the center of the workspace before being used as input for the standard scheme for mobile base positioning.

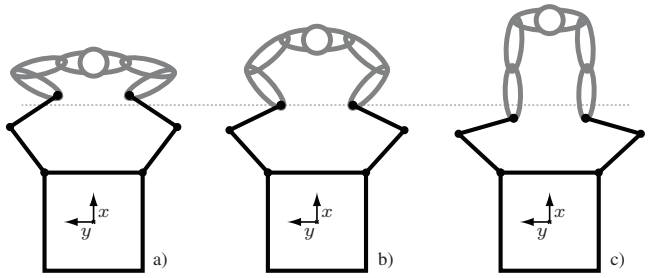

Fig. 8. Mobile base positioning for different arm postures: a) bent arms, b) neutral position, c) extended arms

Including the human arm workspace in the position optimization strategy offers advantages when the operator often makes fast motions using the full workspace of his arms. However, if the operator performs abrupt motions using his legs, the performance can in some cases be deteriorated because the haptic interfaces are operated closer to their workspace limits. Furthermore, it should be noted that including the human arm workspace requires the position of the operator to be tracked. In most application scenarios, the additional effort can be neglected because the position of the operator is already needed to correctly position the teleoperator or avatar.

IV. EXPERIMENTAL RESULTS

In this section, the two discussed methods to calculate the optimal position for the mobile base are evaluated. The following two motion patterns, which represent typical motions in telepresence scenarios, are evaluated:

- operator standing still, moving his arms only
- operator moving, holding his arms in a fixed pose

Typical results are depicted in Fig. 9. It contains the motions of body, mobile base, and the resulting workspace of the haptic displays as well as the true and shifted end-effector positions. Additionally, the unwanted forces at the end-effectors, which are caused by the repositioning motions of the mobile base, are investigated. For the sake of clarity, only one-dimensional motions are evaluated.

A. Operator stationary, arms moving

A common scenario in extensive telepresence is a manipulation task with both arms while standing still. This is reflected by an experiment where the operator stands still. He then stretches out his arms completely and moves them back towards his body as far as possible, thereby using the full range of his arms.

Fig. 9a) shows the base motion when no end-effector position shifting is employed. Consequently, the mobile base travels the full range of the end-effector motions. When

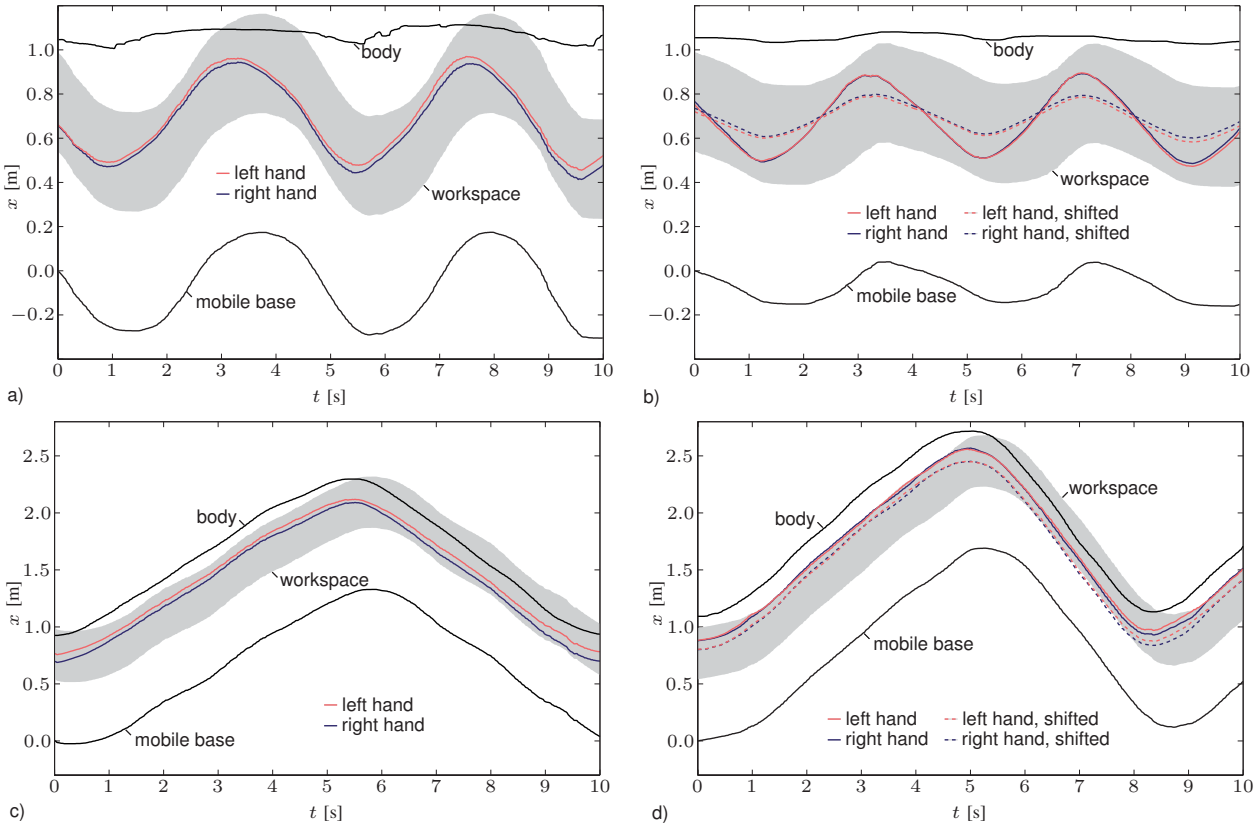

Fig. 9. Comparison of the two base positioning algorithms for two typical motion sequences: (a) Operator moving, arms in fixed pose, no end-effector position shifting. (b) Operator stationary, arms moving, end-effector positions shifted. (c) Operator moving, arms in fixed pose, no end-effector position shifting. (d) Operator moving, arms in fixed pose, end-effector positions shifted. The positive x-direction is aligned with a forward motion of the mobile base pointing towards the operator (cf. Fig. 8.)

shifting the end-effector positions towards the center of the human arm workspace (Fig. 9b), the amplitude of the base motions is significantly reduced. Accordingly, the workspace of the haptic displays ViSHaRD7 is fully used. In conclusion, higher manipulation speeds are possible and less disturbance is felt in the end-effectors.

B. Operator moving, arms in fixed pose

Another interesting scenario is a movement of the body while both arms are held in a fixed pose. This arises for example when carrying objects. Therefore, both hands are held very close to the body during the experiment because heavy objects are naturally carried in this way.

Fig. 9c) shows the results for the case where the actual end-effector positions are directly used as input for the optimization algorithm. When moving in either direction the same distance from the workspace boundaries is maintained and the mobile base moves at the same speed (when the operator moves at the same speed).

Fig. 9d) shows that when the human arm workspace is taken into consideration, i.e. end-effector positions are shifted before optimization, faster motions forward (seen from the viewpoint of the operator) are possible, because the mobile base maintains a bigger distance from the operator ($t = 5 \ldots 8\,\mathrm{s}$). However, backward motions are more limited ($t = 1 \ldots 4\,\mathrm{s}$). Here the workspace boundaries are reached.

C. Unwanted forces during base repositioning

Unwanted forces and torques are felt on the end-effectors during repositioning of the mobile base. This is mainly due to time delays caused by filtering the mobile base position for use in the control loop of the haptic interfaces. To measure this force, the control loop (Fig. 4) is slightly modified: instead of repositioning the mobile base according to the end-effector positions, a predefined trajectory is imposed on the position of the mobile base. The human operator is supposed to hold the end-effector at a fixed position.

Fig. 10 shows the force on one end-effector while the platform moves. Although the magnitude of this force is small compared to the output capabilities of the haptic interfaces, it is large enough to be perceived by the human operator. Thus, slow movements as achieved with the more complex optimization scheme are desirable.

V. CONCLUSION

The hardware and control design of a mobile haptic interface for dual-handed operations in spatially extended environments was presented. In detail, the problem of determining the optimal position of the mobile base was introduced. Two different approaches were elaborated and experimentally tested. In the first approach, only the two end-effector positions are used to calculate a mobile base position for which the two haptic interfaces are operated close to their workspace centers. The second approach also takes the position of the human operator into account. This additional information yields superior results because the operator usually performs much faster motions with his hands

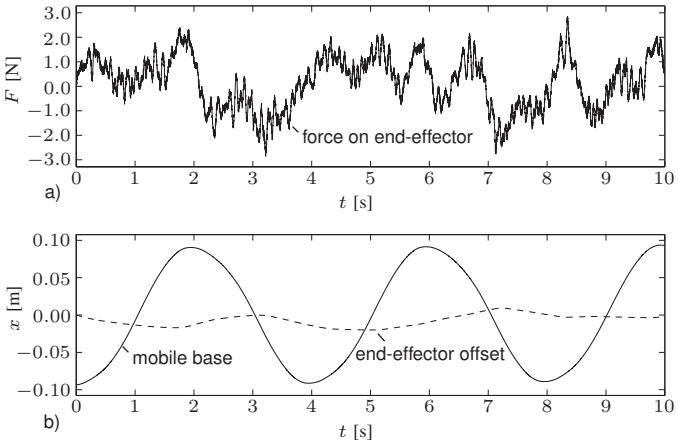

Fig. 10. Force on end-effector during repositioning of mobile base: (a) Measured force. (b) Position of mobile base and offset of end-effector from starting point.

than with the whole body. However, this method requires the relative position between mobile base and operator to be tracked, which increases the hardware effort.

The most serious problem in the current design arises from the non-holonomic nature of the mobile base. This can lead to disadvantageous delays in repositioning the mobile base, which degrade the performance of the optimization algorithm. Therefore, experiments with a holonomic base are in preparation.

VI. ACKNOWLEDGMENTS

This work is supported in part by the German Research Foundation (DFG) within the collaborative research center SFB453 “High-Fidelity Telepresence and Teleaction”. Special thanks to J. Gradl, H. Kubick, T. Lowitz, and T. Stoeber for their excellent work in the construction of the robot.

REFERENCES

[1] N. Bakker, P. Werkhoven, and P. Passenier, “The effect of proprioceptive and visual feedback on geographical orientation in virtual environments,” *Presence: Teleoperators and Virtual Environments*, vol. 8, pp. 36–53, 1999.

[2] U. Künzler and C. Runde, “Kinesthetic haptics integration into large-scale virtual environments,” in *Proceedings of the First Joint Eurohaptics Conference, and Symposium on Haptic Interfaces for Virtual Environment and Teleoperator Systems. World Haptics 2005.*, 2005.

[3] N. Nitzsche, H. U., and S. G., “Design issues of mobile haptic interfaces,” *Journal of Robotic Systems*, vol. 20, no. 9, pp. 549–556, 2003.

[4] M. de Pascale, A. Formaglio, and D. Prattichizzo, “A mobile platform for haptic grasping in large environments,” *Virtual Reality*, vol. 10, pp. 11–23, 2006.

[5] A. Peer, Y. Komoguchi, and M. Buss, “Towards a mobile haptic interface for bimanual manipulations,” in *Proceedings of the IEEE/RSJ International Conference on Intelligent Robots and Systems (IROS)*, 2007.

[6] U. Hanebeck and N. Saldic, “A modular wheel system for mobile robot applications,” in *Proceedings of the IEEE/RSJ International Conference on Intelligent Robots and Systems (IROS)*, Kjongju, Korea, 1999, pp. 17–23.

[7] J.-Y. Wen and L. Wilfinger, “Kinematic manipulability of general constrained rigid multibodysystems,” *IEEE Transactions on Robotics and Automation*, vol. 15, no. 3, pp. 558 – 567, 1999.

[8] N. Klopcar and J. Lenarcic, *Kinematic Model for Determination of Human Arm Reachable Workspace*. Jozef Stefan Institut, Ljubljana, Slovenien, 2005.